New Microwave Antenna Structures for Treating Gastro-Oesophageal Reflux Disease (GERD)

Chris Hancock, *Senior Member, IEEE*, Nuwan Dharmasiri, Christopher I. Duff, *Member, IEEE*, and Malcolm White

***Abstract*—The design and initial pre-clinical evaluation of microwave traveling-wave antenna structures to deliver high-frequency microwave energy with controlled depth of penetration of the electric field to produce controlled ablation around the inner wall of the oesophagus (confined to the mucosal layer) at the junction between the stomach and the oesophagus is described in this paper. The structures were fabricated using flexible microwave substrates to enable them to be attached to the outer wall of oesophageal balloons for introduction into the oesophagus. It is shown that the uniform electromagnetic field produced along the length of the structure produces controlled circumferential tissue ablation, which could be used to tighten the muscles in the lower oesophageal sphincter, where the stomach connects to the oesophagus, to reduce or eliminate regurgitation and acid exposure to the oesophagus, a condition known as gastro-oesophageal reflux disease. This paper also presents the results obtained from *in-vitro* tissue studies and initial *in-vivo* work carried out using the porcine model. This is the first study to assess the use of microwave energy to treat medical conditions associated with the oesophagus.**

***Index Terms*—Gastro-oesophageal reflux disease (GERD), gastroscope, lower oesophageal sphincter (LES), super high frequency (SHF).**

I. Introduction

GASTRO-OESOPHAGEAL reflux disease (GERD) is reflux and regurgitation of the contents of the stomach into the oesophagus (the tube from the mouth to the stomach) and can have a negative impact on daily life. At best, this reflux is uncomfortable, but left untreated, it can cause chronic inflammation and lead to damage and even cancer of the oesophagus.

Food passes from the throat to the stomach through the oesophagus (also called the food pipe or swallowing tube). Once food is in the stomach, a ring of muscle fibers prevents food from moving backward into the oesophagus. These muscle fibers form a valve called the lower oesophageal sphincter (LES), which separates the stomach from the oesophagus. This valve is also known as the antireflux valve. If this sphincter muscle does not close well, food, liquid, and stomach acid can leak back into the oesophagus. This is called reflux or gastro-oesophageal reflux. GERD is one of the most common diseases, with millions of people worldwide experiencing symptoms at least once a month. Over 21 million people in the USA suffer from heartburn or other symptoms of acid reflux two or more times per week. Finely controlled heating of the muscles in the LES, using high-frequency microwave energy delivered from a near-field antenna structure, could offer a clinically preferred solution to tighten and restore the function of the antireflux valve.

The ability to produce controlled circumferential tightening at the LES to restrict the flow of acid from the stomach back up into the oesophagus is challenging due to the location of the LES, the limited thickness of the tissue in this region of the body, which can be less than 2 mm in places [1], and the need to deliver the treatment as quickly as possible to prevent the device from moving (it is only possible to stabilize the patient for a limited amount of time). This paper presents a novel solution to this problem by introducing a center-fed traveling-wave antenna structure that has a width of 5 mm and an overall length of between 40–60 mm that enables controlled near-field propagation of high-frequency microwave energy into the sphincter to produce a band of controlled heating around the sphincter to give controlled tightening. The new structure is mounted onto the outside body of a surgical balloon and introduced through the instrument channel of a gastroscope or cannula in the deflated state, where it can be located, using the camera within the scope, and inflated *in-situ*. A dose of energy of between 8–600 J is delivered in the form of a pulse or burst of microwave power at 14.5 GHz for a duration of between 2–30 s with an amplitude of between 4–20 W to produce a band of controlled heating around the LES with a uniform area and controlled depth of penetration to restrict the flow of juices back up into the oesophagus. The level of control of the heating profile and short treatment time is not possible using other existing treatments.

The new solution uses high-frequency microwave energy generated in the super high-frequency (SHF) band, and a flexible substrate material with a high enough dielectric constant to allow the distance between adjacent slots of the traveling-wave antenna structure to be small enough to produce a uniform band of heating when in contact with biological tissue. The width of the structure is narrow enough to allow the structure to be attached to an oesophageal balloon and be inflated and deflated, and the length is long enough to ensure that at least 270° of the circumference radiates. A frequency of 14.5 GHz ensures that the depth of penetration of the electric field into the tissue produces heating to a depth that does not damage the

Manuscript received October 15, 2012; revised February 22, 2013 and March 15, 2013; accepted March 18, 2013. Date of publication April 15, 2013; date of current version May 02, 2013.

C. Hancock is with the Medical Microwave Systems Research Group, The School of Electronic Engineering, Bangor University, Bangor, Gwynedd LL57 1UT, U.K. (e-mail: c.hancock@bangor.ac.uk).

N. Dharmasiri is with Creo Medical Limited, Bath BA3 4QF, U.K. (e-mail: nuwan@creomedical.com).

C. I. Duff is with the School of Electrical and Electronic Engineering, The University of Manchester, Manchester M13 9PL, U.K. (e-mail: C.Duff@manchester.ac.uk).

M. White is with Creo Medical Limited, Chepstow NP16 5UH, U.K. (e-mail: Malcolm.White@creomedical.com).

Color versions of one or more of the figures in this paper are available online at http://ieeexplore.ieee.org.

Digital Object Identifier 10.1109/TMTT.2013.2256141

muscle layer or cause a perforation, and the insertion loss of the 2.2-mm microwave feed cable that connects the microwave power source antenna is low enough not to cause cable heating. The traveling-wave antenna arrangement comprises of a feed structure, an impedance transformer, and a series of radiating slots in the ground plane. The antenna is fabricated onto a low-loss flexible microwave substrate to allow it to be attached to the surface of a standard oesophageal balloon in a collapsed state to enable it to be introduced into the instrument channel of a gastroscope or a cannula and be expanded when it reaches the LES.

This paper is focused on the design of the new antenna structure and presents initial *in-vitro* and *in-vivo* data gathered to date to demonstrate clinical efficacy. The use of minimally invasive devices, such as the new microwave traveling-wave antenna structure introduced here, offers a clinically attractive alternative solution over other treatment solutions, including medicines (e.g., proton pump inhibitors) and surgery (fundoplication). Other devices that have been considered to treat oesophageal related conditions using minimally invasive techniques and electrical energy include low-frequency microwave or RF devices [2]–[6], but none of these devices offer the level of control of the heating profile and the fast treatment time offered by the new traveling-wave structure.

It has been shown that high-frequency microwave energy generated in the SHF band at a specific frequency of 14.5 GHz can be used to produce fast and controlled ablation of *in-vitro* and *in-vivo*[7], [8] liver tissue. These studies demonstrate the ability to create spherical ablations with a diameter of up to 38 mm (± 1.3 mm) using an omni-directional radiator comprising of a 2.2-mm-diameter rigid coaxial structure with an end-fed radiator with a ceramic tip and integrated quarter-wave impedance transformer [9]. A review of other low-frequency microwave antenna structures designed and developed to address other medical applications is given in [10]–[16].

In the new structure, near uniform heating along the length of the antenna structure, in the near-field, is achieved by controlling the size of the radiating slots within the ground plane. The width of the slots increases with the distance between the generator and the end of the structure. The depth of the heating is a function of the frequency of operation and the tissue type to be treated, i.e., the oesophagus wall. At the chosen frequency, the depth of heating is near ideal for this tissue.

II. Design and Modeling

It is required for the antenna to be designed to be conformal to an oesophageal balloon and fit through the instrument channel of a gastroscope. It should radiate selectively into the oesophagus wall when the supporting balloon is inflated with air or a liquid, i.e., saline solution. A short section of the oesophagus wall around the LES should be heated in order to produce controlled local surface scarring to a controlled depth. It is proposed to achieve this using microwave radiation at a frequency of 14.5 GHz due to the limited depth of penetration of the field.

There are a number of constraints that must be considered.

a) The antenna must be inserted through a tube or channel of approximately 2.5-mm diameter.
b) The antenna must be placed in a known position relative to the wall of the oesophagus (at the LES) so that focused heating can be delivered.
c) It is desired that the heating takes place around at least 270° of the circumference while the antenna is in close contact with biological tissue of high dielectric constant.
d) It is desired to heat the oesophagus uniformly around the circumference.

Constraints c) and d) indicate that the use of an array antenna would be required, but size constraint a) makes this very difficult. Close contact with the oesophagus wall, as required in c), would tend to make a feed network lossy. Constraint a) makes it difficult to include much structure at all, let alone shielding to prevent coupling of the feed to the oesophagus wall.

A traveling-wave antenna structure was considered because it can be designed to distribute its radiation uniformly over its length. If weak coupling is used, the radiation takes place over a large length, and if strong coupling is used, over a short length. The usable length of a traveling-wave antenna may be limited by efficiency considerations because, if the coupling is too weak, more energy may go into losses in the antenna than is radiated.

A. Short Single Traveling-Wave Structure

Electromagnetic (EM) simulations were carried out using CST Microwave Studio to identify the characteristics of transmission lines on the proposed flexible microwave substrate, Rogers R-Flex 3850. It was found that 12.55- and 26.7-Ω lines were of convenient widths, being 1.5 and 0.6 mm wide, respectively. These are close to 12.5 and 25 Ω and are convenient for use in quarter-wave impedance transformers with a transmission line of 50-Ω impedance.

It is desired that transmission should take place in the line without large losses to the oesophagus wall so structures having the ground plane next to the oesophagus were considered. This is because the fields for microstrip are mainly confined close to the track and thus should not couple strongly round to the back of the ground plane, even if the ground plane is only slightly wider than the track. It was found that a layer of oesophagus under the ground conductor of microstrip lines did not significantly affect the transmission loss even for ground planes 2.5 mm wide and track widths of 1.5 mm (12.55 Ω).

A form of traveling-wave antenna that can radiate to the rear of the ground plane was sought. Traveling-wave antennas are matched over a wide bandwidth so that the design is not frequency critical. This is important when the exact characteristics of the load (i.e., the dielectric properties and the spacing from the antenna) are unknown, as a narrowband antenna can be de-tuned if these parameters are different from those assumed in the design, whereas a broadband antenna is more robust to these changes.

There are strong currents on the top of the ground plane directly under the track. These currents mainly flow parallel to the track. A slot in the ground plane, under the track, and transverse to the track, will interrupt these currents and radiate.

An array having 20 transverse slots in the ground plane, centered under the track, was tested. The antenna is shown from the

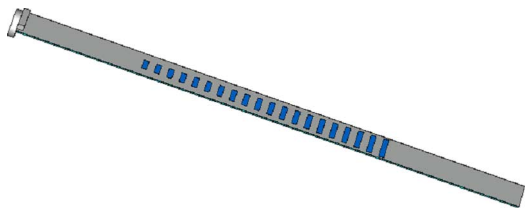

Fig. 1. Traveling-wave antenna with slots in the ground plane.

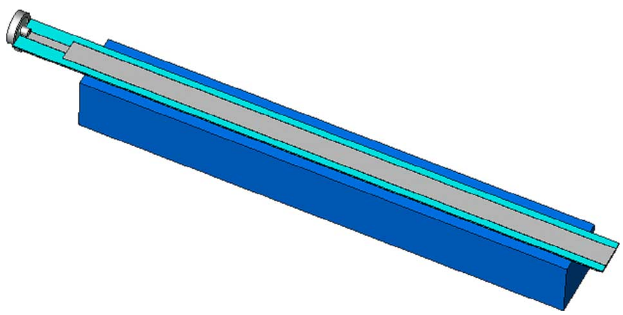

Fig. 2. Antenna seen from feed side with block of oesophagus in contact with radiating side.

TABLE I
LENGTH OF SLOTS FOR SHORT 20-SLOT TRAVELING-WAVE STRUCTURE

Slot number	Slot length (mm)	Slot number	Slot length (mm)
1	0.98	11	1.456
2	1.02	12	1.512
3	1.064	13	1.582
4	1.106	14	1.638
5	1.148	15	1.708
6	1.190	16	1.778
7	1.246	17	1.848
8	1.288	18	1.932
9	1.344	19	2.002
10	1.400	20	2.170

ground-plane side in Fig. 1 and from the feed side, on a block of oesophagus in Fig. 2.

The slots were 0.4 mm wide, with 1-mm increment between slot centers. As a first approximation, slot lengths were chosen that increased in geometric progression along the length of the antenna from 0.98 to 2.17 mm. The array was based on lengths increasing with a common ratio of 1.0405, but with some hand adjustment. In particular, the length of the last element was increased. This is because, as the power remaining in the transmission line falls to a low proportion of the original power, the geometric progression is a poor approximation of the required law. The slot lengths as a function of position along the antenna are given in Table I.

1) Simulation Results From Short Traveling-Wave Structure and Coaxial Transition :

Short Traveling-Wave Structure

The antenna was simulated using CST Microwave Studio. Automatic mesh refinement was used. After four refinements, the result had converged. The return loss of the antenna is shown in Fig. 3. The match between 14–15 GHz is better than 23 dB,

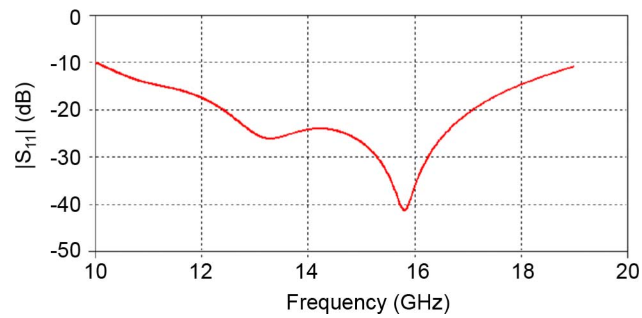

Fig. 3. Input match to antenna fed from 50-Ω line with 25-Ω quarter-wave transformer.

i.e., less than 0.5% of the incident power is reflected back to the load. For the purposes of the simulation, the far end of the antenna was terminated in a matched port so the proportion of power remaining after the last slot is given by s_{21}. The power transmitted past the antenna is smaller than -20 dB from 14 to 15 GHz, i.e., less than 1% of the power remains.

In addition to the return loss and the power transmitted past the antenna, there will also be some ohmic losses in the transmission lines and some losses into the surrounding media. These were assessed by modeling the transmission line without radiating slots and found to give a loss of about 0.6 dB, or 13% of the input power, for a length of transmission line of the same length as this antenna. However, since most of the power has been radiated by the halfway point, the ohmic losses in the antenna might be expected to be half this, i.e., approximately 7% of the incident power. The return loss shown in Fig. 3 is better at 14.9 GHz than at 14.5 GHz, therefore some improvement in efficiency could be obtained if the antenna were redesigned with certain parameters scaled to lower the frequency response by about 2.5%. This might include lengthening the transformer.

Fig. 4 shows plots of power absorbed into the modeled oesophagus wall. These nine plots show the absorbed power density at cross sections taken at 0.1-mm intervals from the antenna center line out to 0.8 mm from the center line. The distance from the center line is shown by the left-hand end of each plot.

The nine plots show that the highest absorption takes place immediately under the coupling slots and that the penetration is of the order of 0.5 mm to the half power point. Within 0.5 mm of the center line, the absorption per slot appears to vary by about 3 dB until the last 1/4 of the length of the array. The power absorption varies only slightly across the antenna cross section out as far as 0.5 mm from the center line. After this, the absorption starts to fall off. At distances more than 0.7 mm from the center line of the antenna, there is little absorption. Some improvement in the uniformity of power absorption along the length of the antenna may be achieved by slightly reducing the lengths of the slots in the center portion of the array. The width over which absorption takes place is determined mainly by the width of the slots and the width of the feed track, whichever is smaller. It is not likely that this can be increased significantly without making the entire antenna wider.

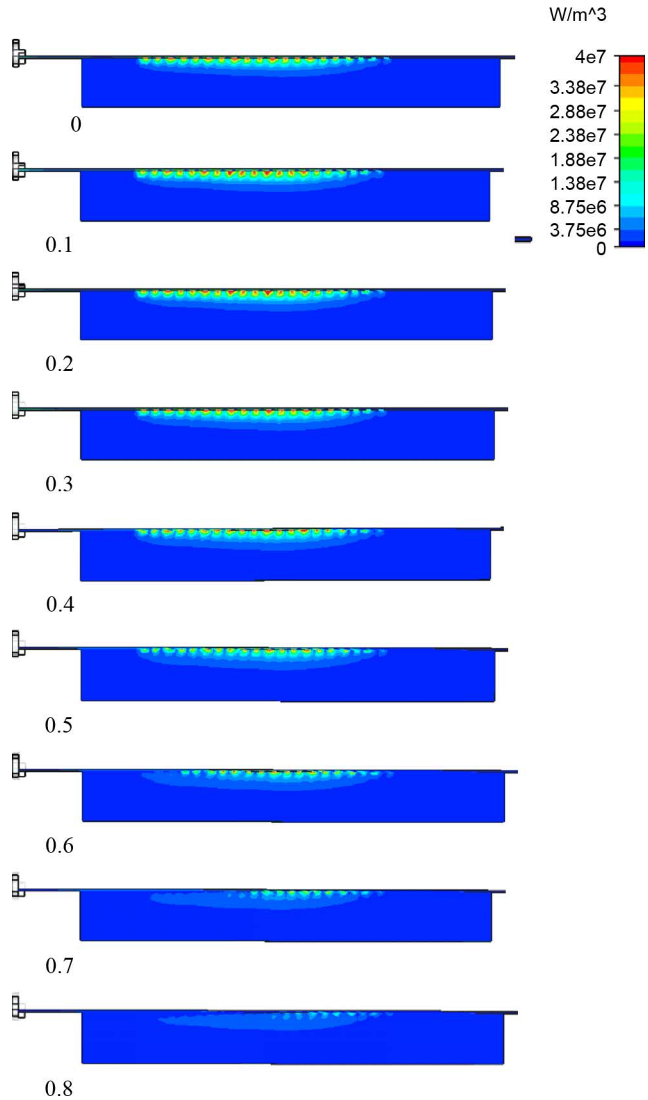

Fig. 4. Power loss density into oesophagus at 0, 0.1, 0.2, 0.3, 0.4, 0.5, 0.6, 0.7, and 0.8 mm from the center plane.

B. Design of the Longer 30-Slot Traveling-Wave Antenna Structure

A longer antenna than the 20-slot traveling-wave antenna described above will be required to allow the device to be used to treat patients that have a large diameter oesophagus. The design of a longer antenna is more difficult than for a shorter antenna so a parametric investigation was carried out and the lengths of the slots were calculated using design equations and interpolated parametric curves.

1) Design Method: A track width of 1.5 mm and a ground plane width of 2.5 mm were used, as in the shorter antenna. The width of the ground plane for the antenna is a compromise between being as narrow as possible and being wide enough to carry all the significant current components on its top face. If it is not wide enough, there would be a small amount of the power flow under the ground plane, which would give additional loss in the oesophagus near both edges of the ground plane. Maximum coupling is obtained by slots that are perpendicular to the current. Under the center of the track, these slots are completely transverse to the track direction. Asymmetric slots could couple if they were longitudinal, but it is expected that the coupling would be quite weak, as the strongest current components are expected to be longitudinal. In order to obtain the strongest coupling, transverse slots running under the center of the track were used. Coupling in the first antenna was varied using the slot length. It is possible that the slot width may also affect the coupling strength.

Variation of Coupling Along the Antenna

In order to obtain uniform power absorption along the antenna, it is necessary to vary the coupling strength along the antenna. If slot n couples a proportion c_n of the power P_n that reaches it, the power coupled at slot n, Q_n, is given by (1) as follows:

$$Q_n = P_n c_n. \tag{1}$$

The power reaching the next slot P_{n+1} will be lower and can be described by (2) as follows:

$$P_{n+1} = P_n(1 - c_n). \tag{2}$$

The power coupled at that slot can then be described by (3) as follows:

$$Q_{n+1} = P_n(1 - c_n)c_{n+1} = Q_n(1 - c_n)\frac{c_{n+1}}{c_n}. \tag{3}$$

In order that the coupled power should remain the same for each slot, i.e., $Q_{n+1} = Q_n$, although the power in the microstrip falls at each slot, it is necessary that the coupling should increase progressively from slot to slot. The slot coupling varies according to the law $(1-c_n)c_{n+1}/c_n = 1$, i.e., $c_{n+1} = c_n/(1-c_n)$. If there are N slots, each slot should couple $1/N$ of the total power so $c_1 = 1/N$. Then $c_2 = 1/(N-1)$ and, in general, $c_n = 1/(N-n+1)$. This assumes that reflections from each slot are small enough to be neglected. Design for good return loss also depends on the reflections from each slot being small and on coherent cancellation between the small reflections from each slot. The return loss is usually also controlled by tapering the start of the antenna, but if uniform coupling is required, as it is here, this cannot be done, so this limits the achievable return loss. If a taper is not used, the return loss depends on the number of slots and the slot spacing.

As each slot is designed to couple a proportion $1/N$ of the power, or more, the power remaining at the end of the array should be of the order of $1/N$ or less. This determines the typical transmission loss. For a 30-slot antenna, the transmission loss should be better than -15 dB.

Determining Slot Lengths and Widths

In order that the first simulation of the array should be close to the desired solution, it is necessary to be able to design slots

TABLE II
COUPLING FOR DIFFERENT VALUES OF SLOT LENGTH AND WIDTH

Slot length (mm)	Slot width (mm)					
	0.2	0.25	0.3	0.4	0.5	0.6
0.2	0.0518	0.0474	0.0475	0.0520	0.0521	0.0522
0.4	0.0504	0.0525	0.0526	0.0514	0.0541	0.0548
0.6	0.0551	0.0549	0.0541	0.0562	0.0578	0.0593
0.8	0.0633	0.0662	0.0679	0.0727	0.0764	0.0806
1.0	0.0842	0.0877	0.0936	0.1006	0.1038	0.1111
1.2	0.1254	0.1336	0.1411	0.1532	0.1646	0.1751
1.4	0.2003	0.2139	0.2320	0.2391	0.2527	0.2726
1.6	0.3155	0.3276	0.3382	0.3532	0.3649	0.3730
1.8	0.4151	0.4238	0.4258	0.4365	0.4451	0.4443
2.0	0.4708	0.4700	0.4723	0.4809	0.4805	0.4807

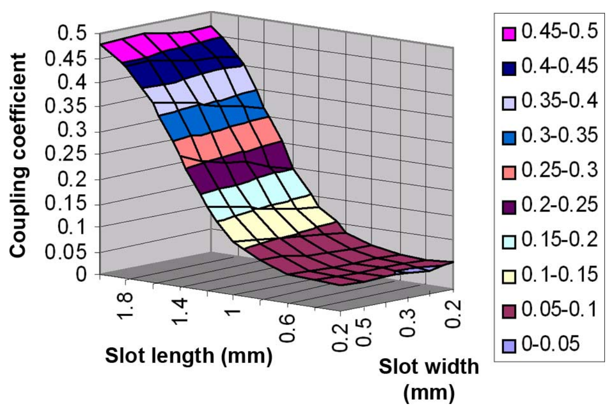

Fig. 5. Variation of coupling with length and width of slot—oblique view.

TABLE III
COUPLING FOR 0.4-mm-WIDE SLOT FOR VARIOUS VALUES OF SLOT LENGTH

Slot length (mm)	S_{11}^2	S_{21}^2	$1-S_{11}^2-S_{21}^2$
0.0	0.000084	0.9527	0.0472
0.05	0.0000	0.9605	0.0395
0.1	0.0000	0.9603	0.0397
0.2	0.0003	0.9609	0.0388
0.4	0.0008	0.9552	0.0439
0.6	0.0019	0.9474	0.0507
0.8	0.0047	0.9287	0.0665
1	0.0108	0.8881	0.1011
1.2	0.0235	0.8100	0.1664
1.4	0.0493	0.6776	0.2730
1.6	0.0882	0.5138	0.3980
1.8	0.1434	0.3814	0.4753
2	0.1779	0.3187	0.5033

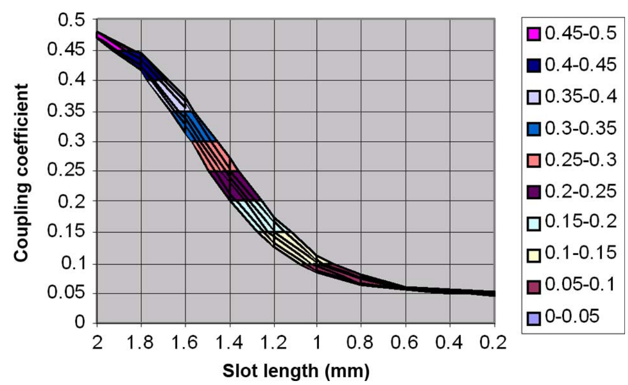

Fig. 6. Variation of coupling with length and width of slot—orthogonal view.

with coupling coefficients that are close to the required values. In order to be able to do this, a large number of simulations of individual slots of different lengths and widths were run using CST. Simulation runs were performed using a short length of microstrip with matched ports at either end. The microstrip had one transverse slot at the center, and loads of a saline balloon and oesophagus over and under the microstrip, respectively. The parametric run option in CST was used so that several lengths were calculated for one width in some simulation runs, and several widths for one length in other runs. Only the length and width of the slots was varied, as the variation of additional parameters, such as track width, would have greatly increased the number of simulations required, and the existing antenna width and impedance are convenient. Simulations were carried out for slot lengths from 0.2 to 2 mm at intervals of 0.2 mm for widths of 0.2, 0.25, 0.3, 0.4, 0.5, and 0.6 mm. In each case, the return loss and the transmission loss were recorded.

The normalized power coupled to the tissue is calculated as

$$C_{w,l} = 1 - s_{11}^2 - s_{21}^2. \tag{4}$$

Table II records the values of normalized coupled power for each slot length and width.

Fig. 5 shows these values in a 3-D format. It can be seen that the width of the slot has very little effect on the coupling. This is confirmed in Fig. 6 in which the surface is seen projected orthogonally to the width axis.

It can be seen that the coupling appears to start at 0.05. This is because dissipative loss in the transmission line has not been taken into account. Allowing for this, the coupling increases roughly as the square of slot length, until the slot length exceeds the track width, 1.5 mm. For longer lengths than 1.5 mm, the coupling increases more slowly with slot length until, at 2-mm length, the coupling is no longer a strong function of slot length. The coupling increases slightly with increasing slot width, but by no more than about 30% for a tripling of slot width from 0.2 to 0.6 mm. Since the coupling is only a weak function of slot width, it was decided to use a fixed slot width of 0.4 mm, as this proved satisfactory for the shorter traveling-wave antenna.

Further predictions were carried out for a slot width of 0.4 mm, for lengths of 0.05, 0.1, 0.2, 0.4, 0.6, 0.8, 1.0, 1.2, 1.4, 1.6, 1.8, and 2 mm. These predictions were carried out with more rigorous conditions for convergence of the adaptive meshing algorithm because the coupling coefficient that is calculated depends on the difference between numbers that are, in most cases, significantly larger than the coupling coefficient, so these numbers need to be accurate. A simulation was also carried out with no slot to determine the dissipative loss. In each case, the return loss and the transmission loss were recorded. The values of s_{11}^2, s_{21}^2, and $1 - s_{11}^2 - s_{21}^2$ for each slot length are shown in Table III.

The dissipative loss in the transmission line was obtained from the transmission and return loss when there was no slot and was found to be 0.0472. This agrees well with the apparent bottom limit of about 0.05 to the normalized coupling coefficient at low slot widths seen in Fig. 6, although it is a little higher

TABLE IV
COUPLING FOR 0.4-mm-WIDE SLOT FOR DIFFERENT VALUES OF SLOT LENGTH—WITH CORRECTION

Slot length (mm)	$1-s_{11}^2-s_{21}^2$	$C_l=1-s_{11}^2-s_{21}^2-a_0$	Polynomial fit
0	0.0472	0.0000	0.0000
0.05	0.0395	0.0015	0.0036
0.1	0.0397	0.0017	-0.0006
0.2	0.0388	0.0008	-0.0006
0.4	0.0439	0.0059	0.0085
0.6	0.0507	0.0127	0.0143
0.8	0.0665	0.0285	0.0254
1.0	0.1011	0.0631	0.0608
1.2	0.1664	0.1284	0.1328
1.4	0.2730	0.2350	0.2374
1.6	0.3980	0.3600	0.3522
1.8	0.4753	0.4373	0.4400
2.0	0.5033	0.4653	0.4613

TABLE V
POLYNOMIAL COEFFICIENTS FOR SIXTH-ORDER BEST FIT TO COUPLING CURVE

Polynomial term	Coefficient
L^6	0.1539
L^5	-1.0832
L^4	2.6546
L^3	-2.744
L^2	1.303
L^1	-0.236
L^0	0.0125

than the lowest coupling values toward the top of the right-hand column of Table III. This is a small inconsistency in the results, despite care having been taken to run the simulations with high accuracy. With no slot, the normalized power returned to the input port, s_{11}^2, was 0.00008, indicating that the port matching to the line was good, and giving confidence in the other results.

To take account of the dissipative losses in the microstrip, the coupling coefficients were recalculated using (5) as follows:

$$C_l = 1 - s_{11}^2 - s_{21}^2 - a_0. \tag{5}$$

These values are shown, together with the old values, in Table IV. Since the lowest coupling values in Table III are less than 0.0472, a value of 0.038 was used for a_0 when calculating the coupling values shown in the third column of Table IV, except for the zero length value. The fourth column of Table IV shows the best sixth-order polynomial fit to the values in the third column. The coefficients of the polynomial are given in Table V.

Fig. 7 shows curves for coupling coefficients calculated using the first set of simulations (First run), the second (more accurate) set of simulations (Longer run) and point-to-point (Empirical) and smooth (Poly) versions of the polynomial approximation. It can be seen that the polynomial is a good fit for coupling values between 0.1–0.4, and couplings of over 0.47 are unattainable.

Fig. 8 shows details of the curves for coupling values between 0–0.1. It can be seen that all the curves are fairly close, but the polynomial fit oscillates a little around the calculated values and is a relatively poor fit for coupling values below 0.15. The curves shown in Figs. 7 and 8, and the associated polynomial, were used as the starting point to design the 30-slot structure.

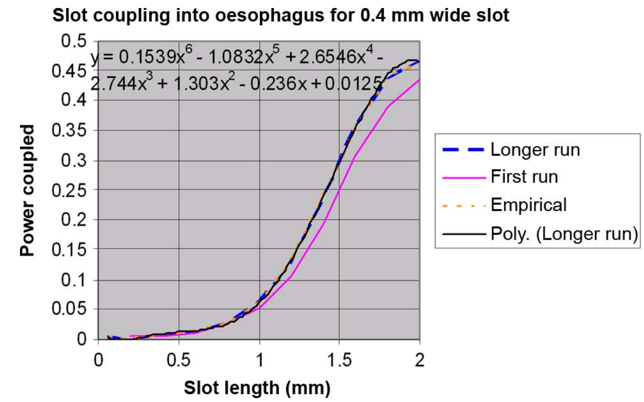

Fig. 7. Variation of coupling with length of slot for width of 0.4 mm.

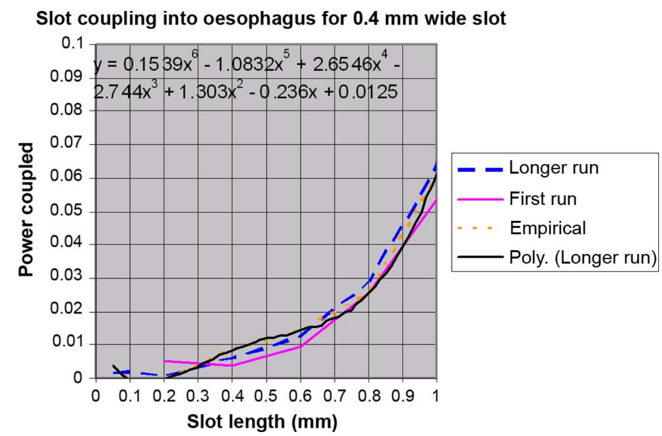

Fig. 8. Variation of coupling with length of slot for width of 0.4 mm: detail at low coupling.

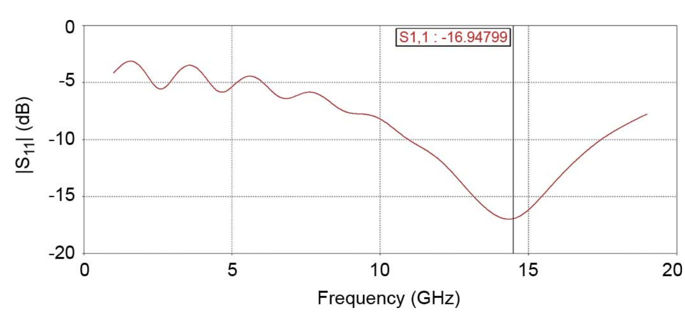

Fig. 9. Return loss for third 30-slot antenna.

The simulated return loss of the antenna with the integrated transition from coaxial cable and transformer is shown in Fig. 9. It can be seen that the match is best at the design frequency. This is mostly due to the transformer characteristics, but interaction between the antenna and the transformer may have resulted in a slight improvement in the return loss at the design frequency. This would depend on the exact distance of the antenna from the transformer.

The simulated transmission loss is shown in Fig. 10. The transmission loss of 30 dB represents only a small proportion of the power coupled at each slot.

The power absorption density is shown in Fig. 11. The absorption close to the beginning of the array is about four times more than near the end of the array. It is noticeable, though,

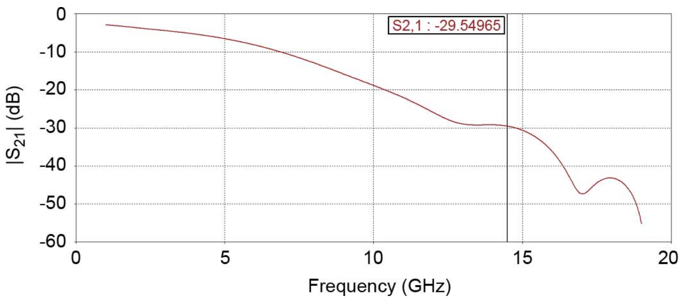

Fig. 10. Transmission loss for third 30-slot antenna.

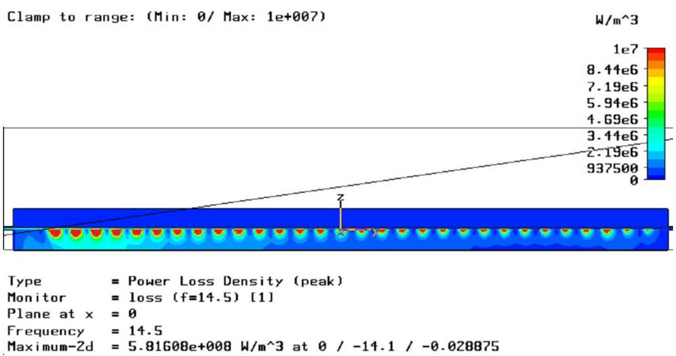

Fig. 11. Power absorption density for third 30-slot antenna.

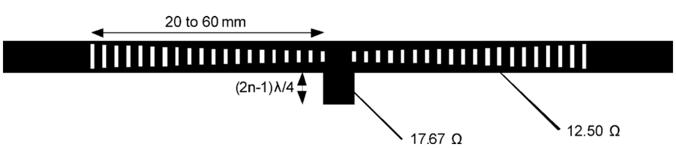

Fig. 12. Two traveling-wave slotted structures connected in parallel, fed by an impedance transformer (ground plane).

that the absorption seems to be fairly constant over most of the last half of the array. This seems to indicate that the coupling is too high for slot lengths less than 1 mm, but about right for slot lengths more than 1 mm. There is a small increase in absorption toward the end of the array, indicating that the coupling may be slightly too high for slot lengths of 1.5 mm or more. It is not clear why this should be. In future work, the predicted coupling needs to be compared with the measured coupling to make sure the predicted variation is real, and then computer optimization used to even out the power distribution in the array.

III. FABRICATION

The substrate material employed for the antennas must be thin and flexible enough to allow the device to be folded and passed through the instrument channel of an endoscope or gastroscope, while the balloon is in its deflated state, and opened up to form a circumferential band in the inflated state. The most suitable material was found to be the Rogers R/flex 3850 substrate with a thickness of 0.002 in (50 μm) and 1/2 oz (18 μm) electrodeposited copper on both sides.

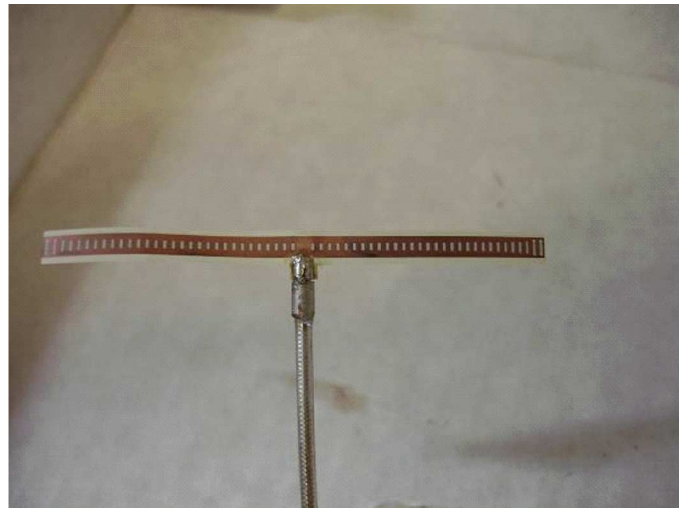

Fig. 13. Fabrication of two 30-slot traveling-wave "T" structures—radiating slots in ground plane.

Fig. 14. "T" structure attached to the outer wall of an oesophageal balloon catheter.

To enable the radiating band to cover at least 270° of the circumference of the oesophageal balloon, two of the long 30-slot structures were used and connected in a "T" arrangement, as shown in Fig. 12 for 20-slot antennas, where the two structures are electrically connected in parallel.

Two 30-slot structures connected in a "T" configuration, fabricated on R/flex 3850 substrate, and connected to a Sucoform 86-cable assembly is show in Fig. 13.

These structures were then attached to the outer wall of the balloon using 0.21-mm polyester carrier double-sided acrylic tape and the microwave cable and the coaxial transition were attached to the balloon using a medically approved Loctite adhesive. Figs. 14 and 15 show the traveling-wave structure connected to the outer wall of the balloon, with the balloon in the expanded state.

It was necessary to find a suitable adhesive to attach the antenna to the balloon. Both Loctite and Araldite adhesives were applied and tested for suitability. It was found that Loctite gave

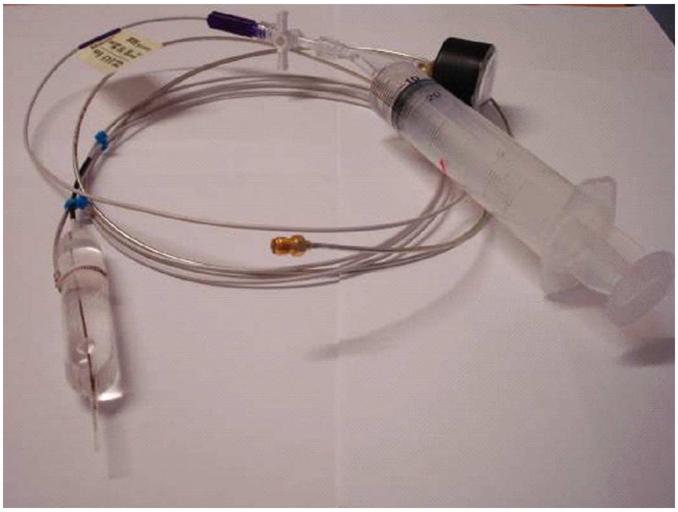

Fig. 15. Antenna structure attached to an inflated balloon with means of inflating and deflating.

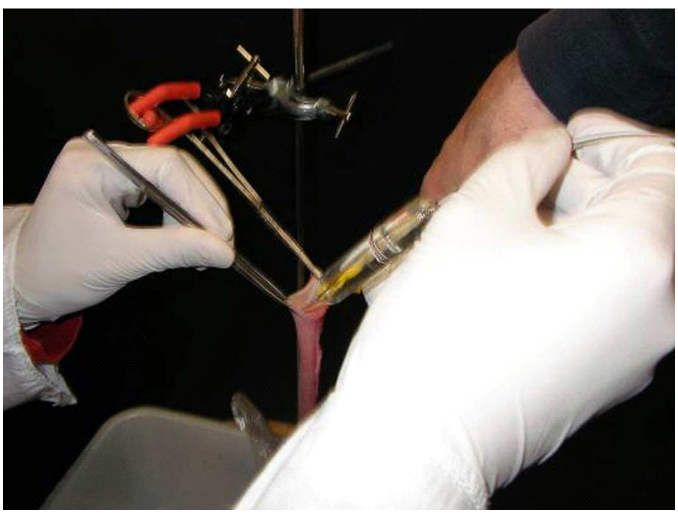

Fig. 16. Prototype antenna structure attached to an inflated balloon being inserted into a porcine oesophagus.

the best results with a solid bond generated between the cable assembly and the surgical balloon.

It was also apparent that the electric field is a maximum at the 1/4-wave T-feed launch junction. It was important to monitor the coupling degradation effects on the overall S_{11} measurements resulting from using Loctite adhesive in the bonding process and the effect of having a double-sided acrylic tape. Any nonuniform application of adhesive underneath the launch feed line might cause a nonuniform field distribution at the junction, thus causing an impedance mismatch at the junction.

IV. Experimental Validation

The prototype device was tested using *in-vivo* and *in-vitro* porcine tissue models. For the *in-vitro* testing, porcine oesophagus models were obtained from a abattoir and the traveling-wave "T" structures attached to an inflated balloon were directly inserted into the oesophagus, as shown in Fig. 16.

A 14.5-GHz generator was used to supply the microwave energy to the antenna structure. The generator was configured

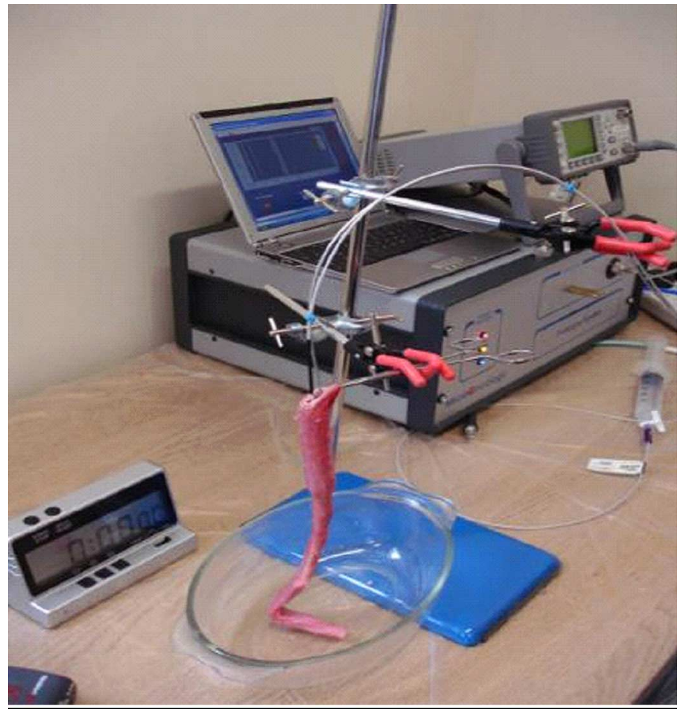

Fig. 17. Experimental arrangement showing a section of a pig's oesophagus with the antenna inserted inside.

to deliver pulses of microwave energy of duration between 1–100 s, and amplitude (measured at the output of the generator) of up to 50 W. A PID controller was used to ensure that the power level was kept constant for the duration of the pulse. Power level and pulse length was set up using a user menu, and the energy was delivered by depressing a foot-switch pedal. The experimental setup used is shown in Fig. 17.

In-Vitro Study

The balloon was inflated to a diameter of 16.25 mm and the traveling-wave antenna was attached using double-sided tape, as shown in Fig. 18. The microwave energy was fed into the antenna using a 1.2-m Huber-Suhner Sucoform 86-microwave-cable assembly.

The ablation results for generator output power of 36 W, resulting in input power to the radiating antenna of approximately 4 W, are shown in Fig. 19.

The region where no tissue effect is observed is due to the antenna structure not having radiating slots in this region. This may offer clinical advantage, as this will limit the amount of closure of the sphincter. The three regions of ablation were created using the same antenna, moved along the oesophagus. Table VI gives the power levels and pulse times used to create the three ablations.

It can be seen that tissue ablation occurs in the regions where the radiating slots are present in the traveling-wave antenna structure, and the depth of penetration is well controlled. The portion of the circumference where thermal damage has not occurred is due to the fact that radiating slots were not present in this region. The delivery cable does not get hot enough to cause any collateral damage to healthy tissue.

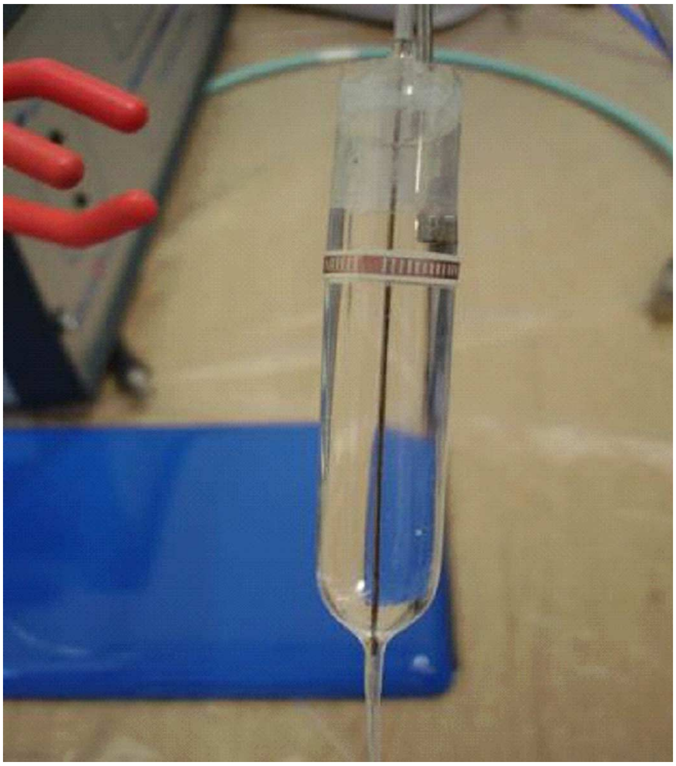

Fig. 18. Antenna structure and medical balloon used in the measurements.

Fig. 19. Oesophagus cut along its length to show three zones of ablated tissue.

TABLE VI
TEST PARAMETERS USED

Power at output of generator:	36W
Power at radiating antenna: approximately	4W
Right hand region of ablation duration	20 seconds
Middle region ablation duration	30 seconds
Left hand region ablation duration	40 seconds

It can be seen that the structures are capable of producing controlled uniform circumferential ablation using a morbid porcine oesophagus model.

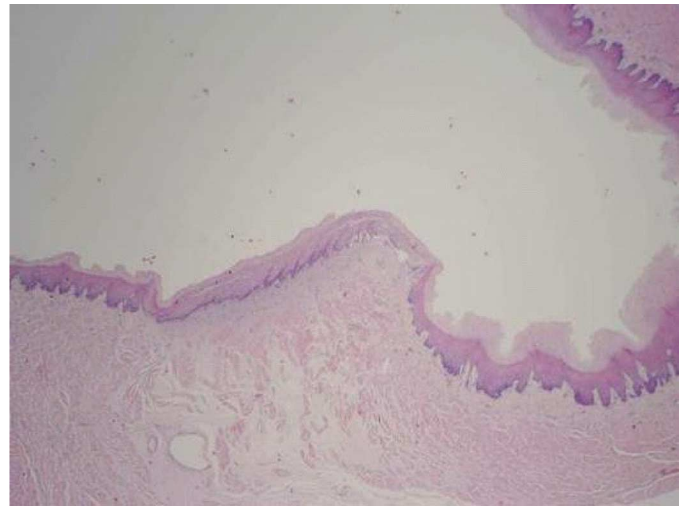

Fig. 20. Porcine model, day 0: H&E stain $\times 20$.

In-Vivo Study

An *in-vivo* study was also carried out using the porcine model. This study was designed to assess the activity of the "T" structure with the potential to ablate mucosa with sub-mucosa, in a controlled manner, in the porcine oesophagus.

The device was passed *per oss* until the tip of the cannula carrying the circumferential ablation antenna was felt or observed just distal to the oesophageal sphincter. The device was then activated and 20 W of power was delivered into the antenna structure for a period of 5 s. The device was then moved proximally 2 cm and activated for a second time using the same power delivery profile, and this was repeated four times to produce four separated ablations of the oesophageal mucosa. The oesophagus was removed and fixed following which histological sections were made of the putative ablation sites.

Two sections from subject C indicated discreet and obvious ablations. With haemotoxylin and eosin stains, shown in Figs. 20 and 21, they are not easy to detect, but are shown as a flattening and a change of orientation together with some loss of integrity of the tissues both at the mucosal side and at the junction of the mucosa with the underlying collagen in this oesophagus. However, using picrosirius red stains, shown in Figs. 22 and 23, it can be seen quite clearly that there is a discreet and obvious delineated area of degraded collagen deep to the mucosa. It is not fully degraded as it still carries small amounts of birefringence, but appears to be at the level that would not survive in a recovery situation.

The positioning of the device to be sure of correct location for ablation was difficult without direct vision, but with a clinical device having remote vision markers this would be overcome. Once in position with the end balloon fully inflated, the device was activated according to "guestimates" of the power required for ablation of oesophageal mucosa. Multi-positioning of the device with the end balloon fully inflated was achieved with ease, which indicates that the inflation of the bladder was probably not sufficient to ensure complete contact between the ablation electrode on the outer circumference of the balloon and the oesophageal mucosa—this could be solved with a larger balloon

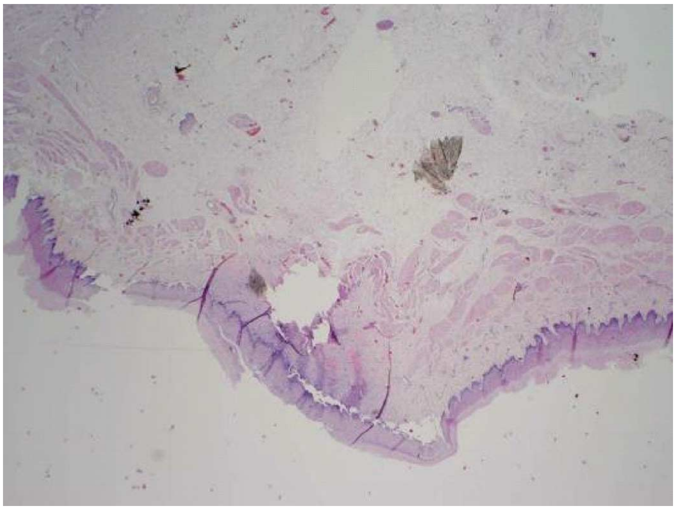

Fig. 21. Porcine model, day 0: H&E stain ×20.

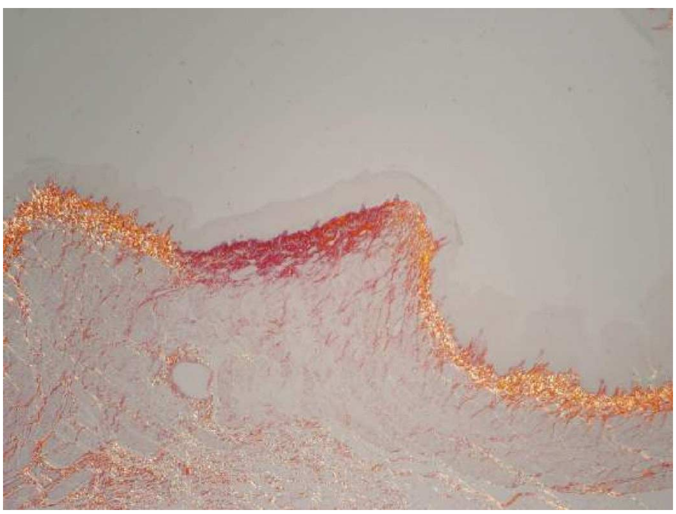

Fig. 22. Porcine model, day 0: picMill ×20 pol.

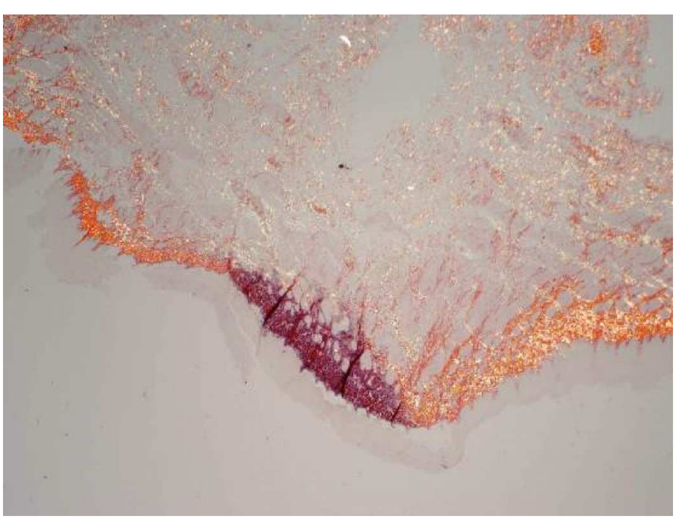

Fig. 23. Porcine model, day 0: picMill ×20 pol.

provide the attached electrode was still active following compliance with deflation and reinflation of the balloon.

Macroscopic examination of the excised oesophagus post ablation showed two obvious ablation sites evidenced by a sharply demarcated whitened areas of the mucosal surface and several other very light "whitenings," which were possible ablation sites. These sites were not complete circumferential changes and seemed to support the probability of the end balloon not being of sufficient size.

The histology also supports this suggestion as the areas seen to be ablated did not form a fully circumferential feature. They were, however, very precise and limited to the mucosa and some of the underlying matrix, but without showing a risk of perforation. This level and depth of ablation is ideal for the adjustment of oesophageal sphincter diameter as a potential reduction of reflux strategy, although the contact been microwave application antennae and the mucosal surface would probably have to be significantly more complete than seen in this initial pre-clinical assessment. The width of the ablation antenna will be the other variable for this type of device, and although there will probably be a mean acceptable width, it is believed that there will be situations that could require thin and/or thick bands of ablation to achieve the required clinical end point.

V. Conclusion

This paper has described the design, EM modeling, fabrication, and initial pre-clinical evaluation of new novel microwave traveling-wave antenna structures that may provide a clinically superior solution for treatment of GERD. It has been shown that the structures can produce near-field propagation of high-frequency microwave energy with a controlled depth of penetration of the electric field to produce well-defined circumferential heating (or controlled ablation) around the inner wall of the oesophagus, just distal to the oesophageal sphincter. The structures were fabricated using flexible microwave substrates to enable them to be attached to the outer wall of oesophageal balloons for introduction into the oesophagus through a tube or cannula. It has been shown that the uniform EM field produced along the length of the structure produces controlled circumferential tissue ablation using a morbid or *in-vitro* porcine tissue model.

A design method has been formulated, refined, and followed to enable traveling-wave antenna structures to be produced that can deliver energy into the wall of the oesophagus to produce controlled ablation of the mucosal layer.

The *in-vivo* study has enabled us to demonstrate that ablation occurs in the region where the radiating slots are present in the ground plane of the traveling-wave antenna structure and the depth of penetration is well controlled. It has also been demonstrated that the microwave cable that delivers the energy from the source to the antenna does not get hot enough to cause any collateral damage to healthy tissue. In the *in-vivo* study, the traveling-wave antenna device delivered the correct intensity of ablation to the oesophageal mucosa, which may make it a viable candidate for use in the treatment of GERD. Having said this, the contact between antenna and mucosa was intermittent and would need to be more complete circumferentially. The principle of the new traveling-wave device has been proven and the results suggest relatively straight forward routing to definitive pre-clinical trials and thereon to clinical use.

A patent application has been filed for this device [17].

ACKNOWLEDGMENT

The authors would like to thank the following people and organizations for their help and support: MDI Limited, Dr. K. O'Goshi, Dr. M. Booton, Dr. J. Bishop, Dr. S. Chaudhry, Prof. P. Sibbons, Dr. P. Wall, and Mr. M. Jarman. The authors would also like to thank Dr. A. Ellis for his time to discuss the various prototype antenna designs and for his clinical input during the development of the prototype GastroBlate system. The intellectual property associated with the traveling-wave antenna structure is owned by MDI Limited.

REFERENCES

[1] F. Xia, J. Mao, J. Ding, and H. Yang, "Observation of normal appearance and wall thickness of oesophagus on CT images," *Eur. J. Radiol.*, vol. 72, no. 3, pp. 406–411, Dec. 2009.

[2] S. D. Edwards and D. S. Utley, "GERD treatment apparatus, and method," U.S. Patent Appl. US 2003/0009165A1, Jan. 9, 2003.

[3] R. A. Stern, R. A. Ganz, and B. D. Zelickson, "System and method for treating abnormal tissue in an organ having a layered tissue structure," U.S. Patent US2004087936A1, May 6, 2004.

[4] J. Jackson and R. A. Stern, "Methods and systems for determining pphysiological characteristics for treatment of the oesophagus," U.S. Patent Appl. US 2003/0215235A1, Oct. 28, 2004.

[5] R. Ganz, B. D. Zelickson, R. A. Stern, J. Jackson, and G. H. Smith, "System and method for treating epithelium in an oesophagus," U.S. Patent Appl. US 2004/0215296A1, Oct. 28, 2004.

[6] R. A. Stern, J. Jackson, V. N. Sullivan, G. H. Smith, R. D. Corbitt, J. A. Hodor, and C. A. Shellenberger, "Devices and methods for treatment of luminal tissue," Int. Pub. #WO 2005/067668 A2, Jul. 28, 2005.

[7] C. P. Hancock, S. M. Chaudhry, P. Wall, and A. M. Goodman, "Proof of concept percutaneous treatment system to enable fast and finely controlled ablation of biological tissue," *Med. Biol. Eng. Comput.*, vol. 45, no. 6, pp. 531–540, Jun. 2007.

[8] R. P. Jones, N. R. Kitteringham, M. Terlizzo, C. P. Hancock, D. Dunne, S. W. Fenwick, G. J. Poston, P. Gheneh, and H. Z. Malik, *Int. J. Hypertherm.*, vol. 28, no. 1, pp. 43–54, Feb. 2012.

[9] C. P. Hancock, N. Dharmasiri, A. Goodman, and M. White, "The design and development of a multi-functional microwave antenna structure for biological applications," *IEEE Trans. Microw. Theory Techn.*, vol. 61, no. 5, May 2013.

[10] A. Rosen, M. A. Stuchley, and A. V. Vorst, "Applications of RF/microwaves in medicine," *IEEE Trans. Microw. Theory Techn.*, vol. 50, no. 3, pp. 963–974, Mar. 2002.

[11] P. Cresson, C. Ricard, N. Bernardin, L. Dubois, and J. Pribetich, "Design and modeling of a specific microwave applicator for the treatment of snoring," *IEEE Trans. Microw. Theory Techn.*, vol. 54, no. 1, pp. 302–308, Jan. 2006.

[12] Z. Gu, C. M. Rappaport, P. J. Wang, and B. A. VanderBrink, "Development and experimental verification of the wide-aperture catheter-based microwave cardiac ablation antenna," *IEEE Trans. Microw. Theory Techn.*, vol. 48, no. 11, pp. 1892–1900, Nov. 2006.

[13] D. Despretz, J. C. Camart, C. Michel, J.-J. Fabre, B. Prevost, J.-P. Sozanski, and M. Chive, "Microwave prostatic hypothermia: Interest of urethral and rectal applicators combination—Theoretical study and animal experimental results," *IEEE Trans. Microw. Theory Techn.*, vol. 44, no. 10, pp. 1762–1768, Oct. 1996.

[14] K. Saito, Y. Hayashi, H. Yoshimura, and K. Ito, "Heating characteristics of array applicator composed of two coaxial-slot antennas for microwave coagulation therapy," *IEEE Trans. Microw. Theory Techn.*, vol. 48, no. 11, pp. 1800–1806, Nov. 2000.

[15] R. D. Nevels, G. D. Arndt, G. W. Raffoul, J. R. Carl, and A. Pacifico, "Microwave catheter design," *IEEE Trans. Biomed. Eng.*, vol. 45, no. 7, pp. 885–890, Jul. 1998.

[16] K. Saito, H. Yoshimura, K. Ito, Y. Aoyagi, and H. Horita, "Clinical trials of interstitial microwave hyperthermia by use of coaxial-slot antenna with two slots," *IEEE Trans. Microw. Theory Techn.*, vol. 52, no. 8, pp. 1987–1991, Aug. 2004.

[17] C. P. Hancock, P. White, and M. White, "Oesophageal treatment apparatus," Eur. Patent Appl. EP2068741 (B1), Aug. 1, 2012, (filed: Oct. 10, 2007).

Chris Hancock (SM'07) received the Ph.D. degree in electronic engineering from Bangor University, Bangor, U.K., in 1996.

From 1997 to 2002, he was a Senior Microwave Engineer with Gyrus Medical Ltd. In 2003, he founded MicroOnclogy Ltd. (now Creo Medical Limited), Chepstow, U.K., to develop his ideas based on dynamic impedance-matching techniques and integrated RADARmeasurement techniques using Ku-band energy for the treatment of breast tumors. In 2009, he was given a personal Chair with the Medical Microwave Systems Research Group, Bangor University. He is also the Chief Technical Officer (CTO) and founder of Creo Medical Limited.

Nuwan Dharmasiri received the Masters degree from Kings College London, London, U.K., in 2000, and the Ph.D. degree from the University of Manchester, Manchester, U.K., in 2006.

In 2007, he joined the Research and Develooment Group, CreoMedical Limited (formerly MicroOncology Ltd.), where he was involved with microwave measurement and calibration techniques for their system. In 2008/2009, his research focused on developing systems combining low-frequency RF and microwave energy. In 2010, he joined the Product Development Team to develop the CRoMa system that comprises bipolar RF and microwave.

Christopher I. Duff (S'05–M'05), photograph and biography not available at time of publication.

Malcolm White received an Honours degree in physics from Exeter University, Exeter, U.K., in 1977.

From 1977 to 1983, he was with the Microwave Tube Division, MO Valve Company [part of GEC (UK)], where he developed miniature magnetrons with small magnetic circuits. From 1983 to 2012, he was with the Radar Cross Section (RCS) Department, Thales UK, as a Microwave Engineer, Trials Engineer, and Mathematical Engineer involved with most aspects of RCS measurement, prediction, analysis, and software design (FACETS RCS prediction software), as well as radar, antenna, filter, and signal processing design. For several years, he was Co-Presenter of The RCS Course and The FACETS Training Course to delegates from industry and government agencies. Since 2012, he has been with CreoMedical Limited, Chepstow, U.K., where he has been involved in the design and development of novel medical tools using microwaves.

Mr. White is a Chartered Physicist. He is a member of the Institute of Physics and the Institution of Engineering and Technology (IET).